REPRT SD-TR-89-28

(4)

Chemical Effects of Ne^+ Bombardment on the $MoS_2(0001)$ Surface Studied by High-Resolution Photoelectron Spectroscopy

J. R. LINCE, T. B. STEWART, M. M. HILLS, and P. D. FLEISCHAUER
Chemistry and Physics Laboratory
Laboratory Operations
The Aerospace Corporation
El Segundo, CA 90245

J. A. YARMOFF
National Institute of Standards and Technology
Gaithersburg, MD 20899

A. TALEB-IBRAHIMI
IBM T. J. Watson Research Center
Yorktown Heights, NY 10598

28 March 1989

Prepared for

SPACE SYSTEMS DIVISION
AIR FORCE SYSTEMS COMMAND
Los Angeles Air Force Base
P.O. Box 92960
Los Angeles, CA 90009-2960

UNCLASSIFIED

SECURITY CLASSIFICATION OF THIS PAGE

REPORT DOCUMENTATION PAGE

1a. REPORT SECURITY CLASSIFICATION Unclassified	1b. RESTRICTIVE MARKINGS
2a. SECURITY CLASSIFICATION AUTHORITY	3. DISTRIBUTION / AVAILABILITY OF REPORT Approved for public release; distribution unlimited.
2b. DECLASSIFICATION / DOWNGRADING SCHEDULE	
4. PERFORMING ORGANIZATION REPORT NUMBER(S) TR-0088(3945-03)-2	5. MONITORING ORGANIZATION REPORT NUMBER(S) SD-TR-89-28
6a. NAME OF PERFORMING ORGANIZATION The Aerospace Corporation Laboratory Operations 6b. OFFICE SYMBOL (If applicable)	7a. NAME OF MONITORING ORGANIZATION Space Systems Division
6c. ADDRESS (City, State, and ZIP Code) El Segundo, CA 90245-4691	7b. ADDRESS (City, State, and ZIP Code) Los Angeles Air Force Base Los Angeles, CA 90009-2960
8a. NAME OF FUNDING / SPONSORING ORGANIZATION 8b. OFFICE SYMBOL (If applicable)	9. PROCUREMENT INSTRUMENT IDENTIFICATION NUMBER F04701-85-C-0086-P00019
8c. ADDRESS (City, State, and ZIP Code)	10. SOURCE OF FUNDING NUMBERS PROGRAM ELEMENT NO. / PROJECT NO. / TASK NO. / WORK UNIT ACCESSION NO.

11. TITLE (Include Security Classification)
Chemical Effects of Ne^+ Bombardment on the MoS_2(0001) Surface Studied by High Resolution Photoelectron Spectroscopy

12. PERSONAL AUTHOR(S)
Linde, Jeffrey R; Stewart, Thomas B; Hills, Malina M; and Fleischauer, Paul D. (continued)

13a. TYPE OF REPORT	13b. TIME COVERED FROM ____ TO ____	14. DATE OF REPORT (Year, Month, Day)	15. PAGE COUNT
		1989 March 28	36

16. SUPPLEMENTARY NOTATION
4 X 10 to the 14th power 4 X 10 to the 16th power

17. COSATI CODES		
FIELD	GROUP	SUB-GROUP

18. SUBJECT TERMS (Continue on reverse if necessary and identify by block number)
Adhesion; Ion bombardment; Molybdenum disulfide (MoS_2); Photoelectron spectroscopy; Solid lubrication; Sputtering

19. ABSTRACT (Continue on reverse if necessary and identify by block number)

The effect of 1-keV Ne^+ bombardment on the clean MoS_2(0001) -1 × 1 surface with fluences between 4×10^{14} and 4×10^{16} Ne^+/cm^2 was studied using high-resolution photoelectron spectroscopy excited with synchrotron radiation. Spectra of the Mo-3d and S-2p core levels were measured with photon energies that ensured that the kinetic energy of their photoelectrons was the same, resulting in the same depth being probed for both core levels. For lower fluences (i.e., $\lesssim 2 \times 10^{15}$ Ne^+/cm^2), S vacancy defect formation occurs in the MoS_2 lattice, with the concurrent formation of a small amount (<10%) of dispersed elemental molybdenum [Mo(0)]. For fluences greater than $\sim 1 \times 10^{16}$ Ne^+/cm^2, the [Mo(0)] is the predominant species in the surface region, while the remaining species consist of amorphous MoS_x ($2 > x$) and polysulfide species. Valence band spectra taken with photon energies of 152 eV and 225 eV were consistent with the core level results. The movement of the valence band maximum toward the Fermi level indicated the formation of a metallic surface region.

20. DISTRIBUTION / AVAILABILITY OF ABSTRACT	21. ABSTRACT SECURITY CLASSIFICATION
☒ UNCLASSIFIED/UNLIMITED ☐ SAME AS RPT. ☐ DTIC USERS	Unclassified
22a. NAME OF RESPONSIBLE INDIVIDUAL	22b. TELEPHONE (Include Area Code) / 22c. OFFICE SYMBOL

DD FORM 1473, 84 MAR 83 APR edition may be used until exhausted. All other editions are obsolete.

SECURITY CLASSIFICATION OF THIS PAGE
UNCLASSIFIED

12. PERSONAL AUTHORS (Continued)

(The Aerospace Corp); Yarmoff, Jory A. (National Institute of Standards and Technology); and Taleb-Ibrahimi, Amina (IBM T. J. Watson Research Center)

18. SUBJECT (Continued)

Neon

19. ABSTRACT (Continued)

Annealing the sample temperatures up to 1000 K resulted in the formation of metallic Mo coexisting, in approximately equal amounts, with reformed MoS_2 in a surface with no long-range order as determined by LEED. Finally, a qualitative depth distribution of the chemical species present after Ne^+ bombardment was determined, by varying the photon energies used for the core level spectra. The results indicate that the preferential sputtering of sulfur over molybdenum occurs predominantly through a mechanism involving chemical bonding effects, specifically, through the preferential emission of polysulfide ions over other species in the bombarded region.

PREFACE

This work was supported predominantly by Air Force Systems Command, Space Division, contract number F04701-85-C-0086. Research was carried out in part at the National Synchrotron Light Source, Brookhaven National Laboratory, which is supported by the U.S. Department of Energy, Division of Materials Sciences and Division of Chemical Sciences (DOE contract number DE-AC02-76CH00016). The authors would like to thank the staff at the National Synchrotron Light Source for their assistance, Dr. S. M. Davis for sharing unpublished results, and Dr. S. Didziulis for helpful comments.

CONTENTS

FIGURES

I. INTRODUCTION

The wide interest in the fundamental and applied properties of MoS_2 is mainly due to its two-dimensional, layered structure. This anisotropy is associated with the exceptional inertness of the $MoS_2(0001)$ -1 × 1 surface. Bombardment of the $MoS_2(0001)$ surface with noble gas ions in order to increase surface reactivity has been well studied [1-7]. These investigations are discussed in relation to their application to lubrication and catalysis elsewhere [1,4,7].

Most of the studies involving ion bombardment (IB) of MoS_2 have used Ar^+ of varying energies as the incident ion. However, Davis and Carver [6] recently studied bombardment of the $MoS_2(0001)$ surface with 1-keV Ne^+ ions. Using ion scattering spectroscopy (ISS), they found an approximately linear correlation between the reduction in the S/Mo ratio and the amount of oxygen that could be chemisorbed on the surface. They concluded that this was due to the creation of S surface vacancies for fluences of 10^{15}-10^{16} Ne^+/cm^2. Also in that study, it was found that Ne^+ bombardment did not produce any metallic Mo as determined by x-ray photoelectron spectroscopy (XPS). The only effect of ion bombardment on the Mo-3d doublet was to broaden it slightly. There were no apparent Mo or S peak shifts, even for ion doses of ~ 1 × 10^{18} Ne^+/cm^2. In a subsequent study [8], Davis and Carver found that bombardment did produce shifting of the core level peaks to lower binding energy and peak broadening, similar to effects observed for 10-keV Ar^+ [1]. In order to determine whether this behavior is due to band-bending and inhomogeneous broadening [1] or, rather, to production of reduced molybdenum species, it is necessary to investigate the noble-gas-ion bombardment of the $MoS_2(0001)$ surface in greater detail, i.e., with instrumentation that has greater resolution and surface sensitivity.

Photoelectron spectroscopy that uses synchrotron radiation as the excitation source is ideal for determining how low-energy ion bombardment affects the chemical state at the surface region. The ability to tune the

photon energy allows one to ensure that the kinetic energies of core level photoelectrons resulting from different species in the material are the same. Therefore, the same depth may be probed for all species studied in the experiment. In addition, the spectra may be repeated with higher or lower electron kinetic energies in order to determine how the relative amounts of the chemical species change with the depth probed. This can result in a qualitative "depth distribution" of the various chemical species in the surface region. The purpose of the present study is to utilize synchrotron radiation, in conjunction with a high-resolution electron energy analyzer, to resolve current controversy on the effect of bombardment of the $MoS_2(0001)$ surface with low-energy Ne^+ ions and, in general, to investigate the chemical effects of ion bombardment in greater detail than has heretofore been attempted.

II. EXPERIMENTAL

The present study was performed at beam line U8-B at the National Synchrotron Light Source at Brookhaven National Laboratories. Clean basal plane surfaces were produced by cleavage of natural molybdenite crystals (supplied by Ward's Natural Science Establishment, Rochester, NY). The crystals were cleaved in air and mounted on a sample holder such that their edges were held between two Ta clips for heating in vacuum. The samples could be introduced into the preparation and spectrometer system through a load lock. The preparation chamber (~ 1×10^{-10} Torr base pressure) was equipped with a Microscience rear-view low-energy electron diffraction (LEED) system and a Physical Electronics ion bombardment gun. The sample preparation chamber was connected to the spectrometer chamber (~ 3×10^{-11} Torr base pressure), so that the sample could be maintained under ultrahigh vacuum (UHV) conditions during transfer between ion-bombardment and analysis steps.

After installing samples in the sample preparation chamber, they were heated to ~ 750 K for 10 min to drive off adsorbed hydrocarbons (air-cleaved samples typically have ~ 0.2 monolayers (ML) of hydrocarbons physisorbed on their surface, with no measurable oxygen-containing species [1]). This annealing procedure is known to remove virtually all contamination from the surface without formation of defects [9,10]. Photoemission showed no evidence of either carbon, oxygen, or other impurities on the sample after the anneal, while LEED showed good quality (0001) -1 × 1 patterns.

Ne^+ (and Ar^+) ion bombardment was accomplished by valving off the ion pump, backfilling the chamber with ~ 2×10^{-5} Torr of the gas (Research grade: 99.999% purity) and cycling the titanium sublimation pump. The Ne gas was passed through a bent copper tube immersed in liquid nitrogen in order to condense water and other background gases prior to leaking it into the chamber. The ion bombardment was performed at an energy of 1 keV and

with current densities of 0.1 - 1.0 $\mu A/cm^2$. The incident ion beam direction was located ~ 5° off of the sample surface normal (the azimuth of this misorientation was not known). The current density was made to vary less than 10% over the sample surface by defocusing the ion beam and mapping out the angular distribution of the ions. The ion current density was measured by assuming a ~ 0.25-cm^2 sample surface area and by measuring the current hitting the sample. In calculating the ion fluence, it was assumed that the emission of secondary electrons was smaller than 1 electron per incident ion for this material and ion energy [11]. These considerations aside, it is assumed that the calculated ion fluences cannot be accurate to better than a factor of about 2, although the precision is probably better than ~ 10%.

The energy of the synchrotron light was tuned using a 10-m toroidal grating monochromator (described previously [12]), employing a grating whose energy width and photon intensity were optimum for the range of photon energies used in this study. An ellipsoidal mirror analyzer that was used in an angle-integrated mode (described in Ref. 13) was used to collect the electron energy distribution curves for both core level and valence band spectra. The instrument resolution is demonstrated by the nearly complete separation of the j = 1/2 and j = 3/2 components of the S-2p doublet for the cleaved MoS_2(0001) surface in Fig. 1f (page 15). The instrumental resolution was estimated to be 0.3 eV, 0.4 eV, and 0.5 eV at photon energies of 230 eV, 300-330 eV, and 400 eV, respectively. The S-2p core levels were collected for $h\nu$ = 230 and 330 eV, while the Mo-3d core levels were collected for $h\nu$ = 300 and 400 eV. The low-and high-photon energy excitations for each species correspond to ~ 70-eV and ~ 170-eV electron kinetic energy, respectively. This ensured that the same escape depth was used for sampling both the S and the Mo, while the use of two different electron kinetic energies for each pair of S/Mo core levels resulted in the ability to perform a qualitative "depth profile" of the chemical species present within the top 10-15 Å of the surface region, since ~ 70- and~170-eV electrons are estimated to correspond to an inelastic mean free path (IMFP) of ~ 3.5 and ~ 6 Å , respectively [14].

The relative intensity of the monochromatized synchrotron radiation was determined by measuring the total current resulting from the electron emission from the (carbon contaminated) Au-coated final focusing mirror with an electrometer. The spectra were normalized by dividing the photoelectron current by the photon intensity determined in this manner in order to cancel the effects of variation in the beam current. Although the normalization was adequate for correcting for these small relative changes during the collection of one spectrum, it was not considered accurate enough to allow comparison in the changes of relative intensities between spectra of two different core levels. Therefore, the present study did not determine the change in the S:Mo ratio. However, previous studies using XPS [1,2] and Auger electron spectroscopy (AES) [2,4,5] have shown that this ratio drops by a factor of as much as 2.5 in the surface region (top ~ 5-15 Å) for both Ar^+ and Ne^+ bombardment and for ion fluences of ~ 1×10^{16} Ne^+/cm^2, although relatively little depletion occurs for bombardments less than ~ 1×10^{15} Ne^+/cm^2.

Core level spectra, in addition to having good resolution, exhibited good signal-to-noise characteristics and, therefore, were very amenable to peak-fitting. The spectra were fitted on a VAX 11/780 computer using a fitting program based on Bevington's CURFIT [15]. The functional form used for the fits consisted of Voigt functions approximated by Gaussian quadrature. The background was approximated by a combination of an "S-shaped curve" [16] and a straight line with variable slope. For fitting the Mo-3d doublet, the peak separation and the relative area ratio for the 5/2 and 3/2 spin-orbit components were constrained to be 3.14 eV and 1.43, respectively, while the corresponding constraints for the S-2p 3/2 and 1/2 spin-orbit components were 1.19 eV and 2.01.

III. RESULTS AND DISCUSSION

A. CORE LEVEL RESULTS

Mo-3d and S-2p core level photoelectron spectra of a cleaved $MoS_2(0001)$-1 × 1 surface, taken with an electron kinetic energy of ~ 70 eV after various stages of Ne^+ bombardment, are shown in Fig. 1 (page 15). All spectra are similar to spectra taken for a sample bombarded by Ar^+ ions, reported elsewhere [3].

The spectra were fit using the procedure described above. The S-2s singlet coincidentally appears at a binding energy (BE) ~ 1.8 eV lower than that for the Mo-$3d_{5/2}$ doublet and is also included in the fit. If the Lorentzian widths of the peaks were constrained to be equal to the values for the unbombarded surface, then fits of fair quality could only be obtained by using four spin-orbit split doublets for each of the Mo-3d and S-2p spectra. It was found that much higher quality fits could be obtained by allowing the Lorentzian widths to vary in addition to the Gaussian widths, and by using only two doublets for the Mo-3d spectra and two doublets for the S-2p spectra (except for the 4×10^{16} Ne^+/cm^2 case, which required at least three doublets). The change in the Lorentzian widths can be explained by final state relaxation effects as the crystallinity of the surface region changes with ion bombardment. The results of peak fitting are superimposed over the spectra, while the deconvolution into individual peaks is shown below the data.

With initial Ne^+ bombardment of 4×10^{14} Ne^+/cm^2, the Mo-3d spectrum (Fig. 1b) shows the appearance of a species at ~0.6 eV lower BE than for the Mo(IV)-MoS_2 species that represents the appearance of a reduced Mo species in the surface region. The relative intensity of this species appears to drop slightly for 2×10^{15} Ne^+/cm^2 (Fig. 1c), and then increases greatly for 1×10^{16} Ne^+/cm^2 (Fig. 1d). For the highest fluence (Fig. 1e), this species represents the predominant Mo species at the surface region. In addition, the binding energy shift increases from 0.6 eV to 0.8 eV from the lowest to the highest fluence (Table I, page 16).

These results clarify a previous study in which ion bombardment of the $MoS_2(0001)$ surface was studied with XPS at lower resolution than in the present study, and these two species were not resolved [1]. The conclusion from that study was that ion bombardment with 10-keV Ar^+ ions caused changes that resulted in downward band-bending of ~ 0.8 eV at the surface. This conclusion is probably in error, since our higher resolution results show that the Mo(IV) doublet does not shift greatly, but reduces in intensity relative to the lower BE Mo-3d doublet. Even though 10-keV Ar^+ ions were used in that study, this is still in the energy range in which the sputtering mechanism would be expected to be similar; also observed was the presence of the reduced Mo species with 1-keV Ar^+ ions [3]. In a preliminary study, we have used a nonmonochromatized Mg-K(α) source to study 1-keV Ne^+ bombardment of $MoS_2(0001)$ (essentially the same conditions as in Ref. 6). The results for a ~ 10^{17} Ne^+/cm^2 bombardment are very similar to those in Ref. 1, showing that most of the Mo is in the form of the reduced species (~ 0.6-eV shift of the Mo-$3d_{5/2}$ peak to lower BE).

The origin of the reduced Mo species is not immediately clear. The BE shift (~ 0.7 eV) between the two Mo species is too small for bulk Mo metal {Mo(MoS_2) - Mo(metal) = 1.1 eV [17], while the shift is probably too large to correspond to Mo(III), as in Mo_2S_3. Determination of the chemical state of the Mo, however, is dependent on analysis of the changes in the S-2p core level.

The bombardment-produced species in the S-2p doublet do not correspond to the bombardment-produced species in the Mo-3d doublet. For all bombardment levels except for the highest one (4×10^{16} Ne^+/cm^2), the major sulfur species appears to be the S(2-) in MoS_2. For the 2×10^{15} and 1×10^{16} bombardments, a small, higher-BE species appears whose area represents only ~ 2% and ~ 6% (respectively) of that for the S(2-) species. For these same fluences, the area of the lower-BE Mo species is ~ 9% and ~ 120% of the Mo(IV) species. This observation, along with the fact that S is depleted in the surface region [2,3], suggests that the lower-BE Mo species is not associated chemically with any sulfur species. Therefore, the

lower-BE Mo species does not occur as a result of compound formation with sulfur.

A probable interpretation of these results is that some of the Mo from the MoS_2 is being implanted into the crystal (~ 10 Å deep) and forming small amounts of zero-valent Mo, or "Mo(0)." The binding energy for the Mo(0) is too high for metallic Mo(0), suggesting that it is present as very small aggregates of Mo, probably consisting of no more than one or a few atoms, dispersed in the MoS_2 matrix. The small size of these aggregates can result in final state effects [18], possibly explaining the smaller-than-expected shift between the Mo(0) and the Mo(IV) doublets. Extra-atomic relaxation (i.e., neutralization of the charged species produced by photoemission) can occur slowly in small metal clusters when adsorbed on or included in materials with low conductivity. This results in an increase in the apparent BE relative to the bulk metal. This is consistent with the decrease in BE of the Mo(0) doublet by about 0.2 eV between the lowest and the highest fluence (see Table I), which indicates that the average size of the Mo(0) aggregates is increasing as fluence increases.

As mentioned above, the evolution of the S-2p spectra indicates that little change in the chemical state of the S occurs for fluences $\lesssim 1 \times 10^{16}$ Ne^+/cm^2. In fact, for $\lesssim 2 \times 10^{15}$ Ne^+/cm^2, the Gaussian width virtually does not change (Table I, page 16) -- the change in peak shape is due to the change in the Lorentzian width -- suggesting that there is little inhomogeneity in the chemical state of the S. A possible explanation for the change in the Lorentzian width is that low levels of ion bombardment caused vacancy defect formation, resulting in changes in the photoemission final state due to electronic changes in the surface region.

For the 2×10^{15} and 1×10^{16} Ne^+/cm^2 bombardments, there is a small amount of an S species that has a BE ~ 1.0 eV higher than the S(2-) species (mentioned above). This shift is approximately that expected for the creation of polysulfide ion [or $(S\text{-}S)^{2-}$] [19]. This shift does not represent elemental sulfur, since that BE is ~ 0.8 eV lower than in the present case [17]. The polysulfide ions may be produced when the Mo is implanted

into (or sputtered from) the lattice. When a Mo atom is removed from the MoS_2 lattice, it leaves three neighboring S atoms with dangling bonds, since they are now each bonded to two Mo atoms rather than three. Two of the atoms can then reconstruct to bond to each other, lowering the oxidation state per atom, resulting in the formation of $(S\text{-}S)^{2-}$ species.

For the highest fluence, i.e., 4×10^{16} Ne^+/cm^2 (see Fig. 1j), a number of oxidation states of S are produced. The resulting S-2p spectrum can be fit fairly well by three doublets. Although it was decided to use three doublets to fit this spectrum, the shape of the S-2p spectrum indicates the existence of two general sulfur states. From the center to the high-BE side of the spectrum, a range of oxidation states exists (represented by the two higher binding energy species). Sulfur with a single oxidation state on the low-BE side is demonstrated by the sharp drop-off on the right as compared to the left side of the spectrum. A reasonable estimate of the identity of the various species is that the low-BE material corresponds to sulfur in an amorphous Mo-S region, i.e., MoS_{2-x}, where $x>0$, while the range to higher BE corresponds to the polysulfide material discussed above, but with a wide range of bonding states to various Mo-containing species in the now amorphized surface region.

Fig. 1e shows that, for 4×10^{16} Ne^+/cm^2, most of the Mo (~80%) is in the form of Mo(0). The remaining Mo is represented by a broadened doublet (see gaussian widths in Table I) that is shifted ~ 0.3 eV to lower BE as compared to stoichiometric MoS_2. This indicates that an amorphous state consisting of MoS_{2-x} has been produced with the Mo, on the average, in a somewhat reduced state.

To summarize this section, 1-keV Ne^+ bombardment of the $MoS_2(0001)$ surface produces a net depletion of sulfur in the surface region, while some polysulfide ion and increasingly larger amounts of Mo(0) are produced. The remaining material consists mostly of amorphous MoS_2 with varying amounts of sulfur vacancy defects.

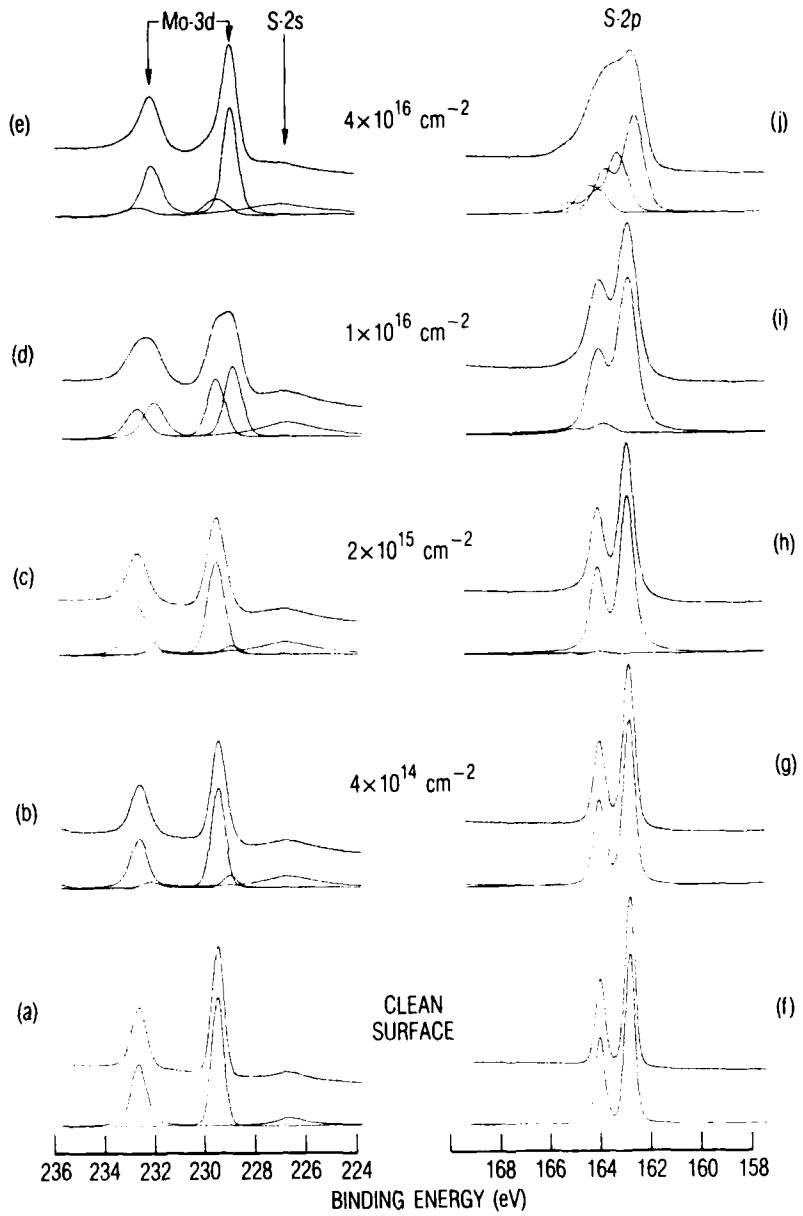

Fig. 1. Mo-3d and S-2p Core Level Spectra for the $MoS_2(0001)$ Surface That Had Been Bombarded With 1-keV Ne^+ Ions. Spectra were taken with photon energies of 300 eV and 230 eV, respectively, which resulted in a photoelectron kinetic energy of ~70 eV in both cases. The S-2s singlet appears on the low-binding-energy side of the Mo-3d doublet. Figs. (a) and (f) are for the clean $MoS_2(0001)$-1 × 1 surface, while (b) and (g) are for a Ne^+ fluence of 4×10^{14} Ne^+/cm^2, (c) and (h): 2×10^{15} Ne^+/cm^2, (d) and (i): 1×10^{16} Ne^+/cm^2, (e) and (j): 4×10^{16} Ne^+/cm^2. Binding energies are relative to E_f.

Table I. Binding Energy Shifts (eV) for the Mo-3d and S-2p Peaks on Ne^+-Bombarded MoS_2(0001) Relative to Those for the Clean Surface[a]

Fluence	Mo-3d		S-2p			Gaussian Widths	
(Ne^+/cm^2)	Mo(IV)	Mo(0)	$(S\text{-}S)^{2-}$	S(2-)	"low-BE S"	Mo(IV)	S(2-)
4×10^{14}	-0.1	-0.6	--	0.0	--	0.37	0.27
2×10^{15}	-0.1	-0.7	+1.0	0.0	--	0.46	0.25
1×10^{16}	0.0	-0.7	+1.0	+0.1	--	0.45	0.40
4×10^{16}	-0.3	-0.8	+1.2 to +0.5	-0.2	--	0.60	0.49
Annealing temperature							
750 K	+0.2	-0.9	--	+0.2	-0.3	0.44	0.32
1000 K	+0.2	-0.9	--	+0.2	-0.4	0.42	0.30
Clean MoS_2(0001)						0.33	0.24

[a]Uncertainty in binding energy changes is ~0.1 eV.

B. VARIATION OF THE VALENCE BAND WITH 1-keV Ne^+ BOMBARDMENT

Fig. 2 shows the valence band spectra taken with a photon energy of $h\nu$ = 152 eV for a clean $MoS_2(0001)$ surface and after bombardments corresponding to two different fluences, while Fig. 3 was produced with $h\nu$ = 224.7 eV for all bombardment fluences used in this study and for the two annealing temperatures. The 152-eV valence band spectrum for the clean surface (Fig. 2a) exhibits structure similar to that for spectra taken in other studies [20,21] except that the relative heights of the peaks are different. This occurs because of the variation in their relative photoelectron cross sections with photon energy. Peaks B-E represent a mixture of Mo-4d- and S-3p-like states in the valence band, peak A represents a state that is predominantly Mo-4d in character (known as the "d_z2" state [21]), and peak F is the S-3s peak. The two peaks visible at 9.3 and 10.5 eV in Fig. 2 represent the S-2p core level doublet produced by second-order light from the monochromator. The spectrum for the 224.7-eV photon energy (Fig. 3a) also has peaks A-F in the same positions as in Fig. 2a. The significance of the 224.7-eV photon energy is that this is where the Mo-3d absorption edge appears, resulting in resonance effects in the valence band spectra [22]. Briefly, the resonance results in peak A being significantly enhanced as compared to peak B, since peak B has less Mo-4d character than peak A [21]. Peaks C and D are also enhanced, but to a lesser degree. The relative enhancements represent correspondingly larger amounts of Mo "d" character in these peaks.

For the off-resonance spectra ($h\nu$ = 152 eV), bombardment results in the area under the valence band (peaks A-E) increasing as compared to the area under the second-order S-2p doublet (also as compared to the S-3s peak or peak F), indicating that the valence band has increasingly greater Mo character as the Ne^+ fluence increases. Fig. 2b represents the 2×10^{15} Ne^+/cm^2 bombardment, which exhibits broadening due to the production of amorphous material in the surface region, but shows relative peak positions that are essentially the same as for clean $MoS_2(0001)$ (Fig. 2a). The peak intensities of A, C, and D are enhanced somewhat compared to peak B (as in

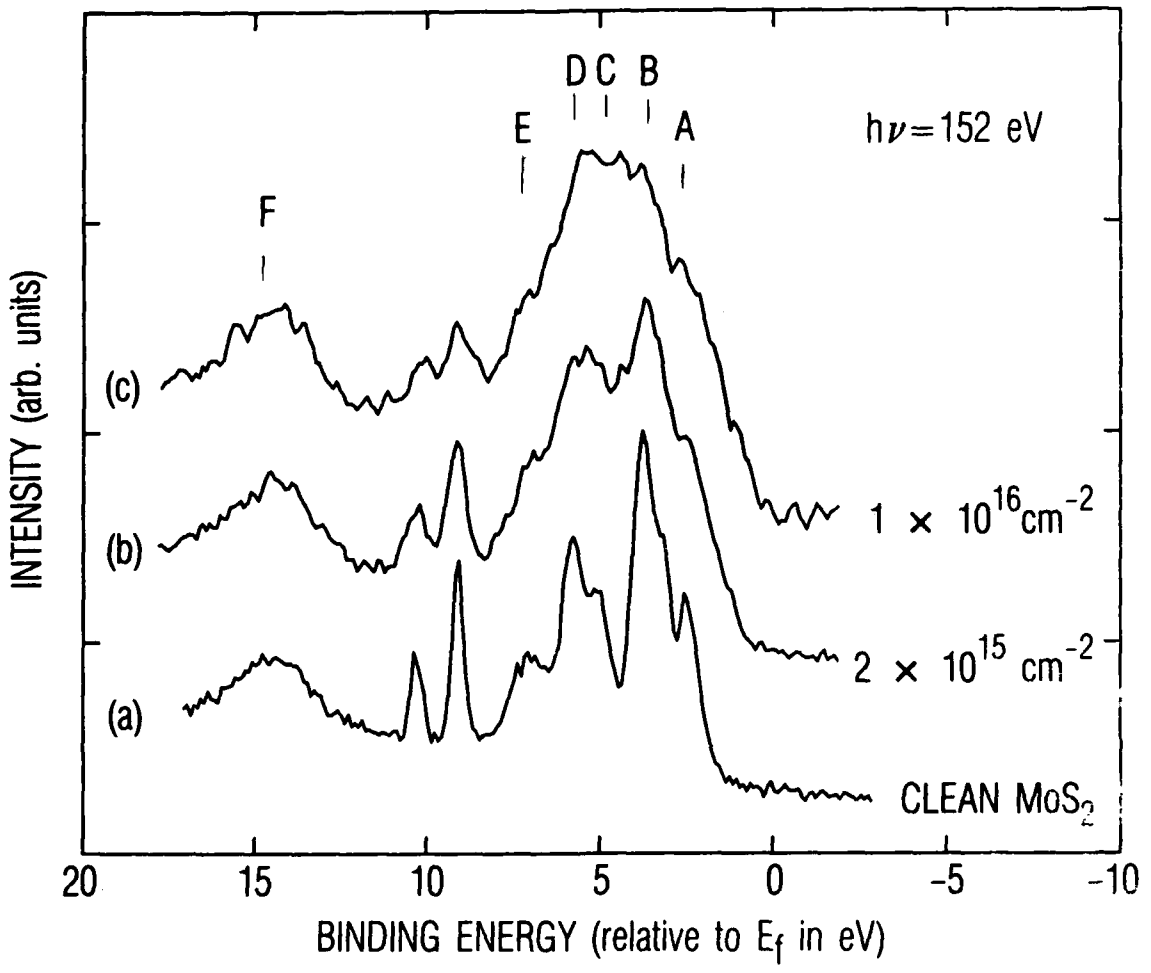

Fig. 2. Valence Band Spectra Taken Using a Photon Energy of 152 eV for (a) the Clean MoS_2(0001)-1 × 1 Surface, and for Surfaces That Had Been Bombarded With (b) 2 × 10^{15} Ne^+/cm^2 and (c) 1 × 10^{16} Ne^+/cm^2. Peak A represents the "d_z2" state, while peaks B-E represent a mixture of Mo-4d- and S-3p-like states. Peak F is the S-3s peak. The two peaks visible at 9.3 and 10.5 eV result from the S-2p core level doublet produced by second-order light from the monochromator. Binding energies are relative to E_f.

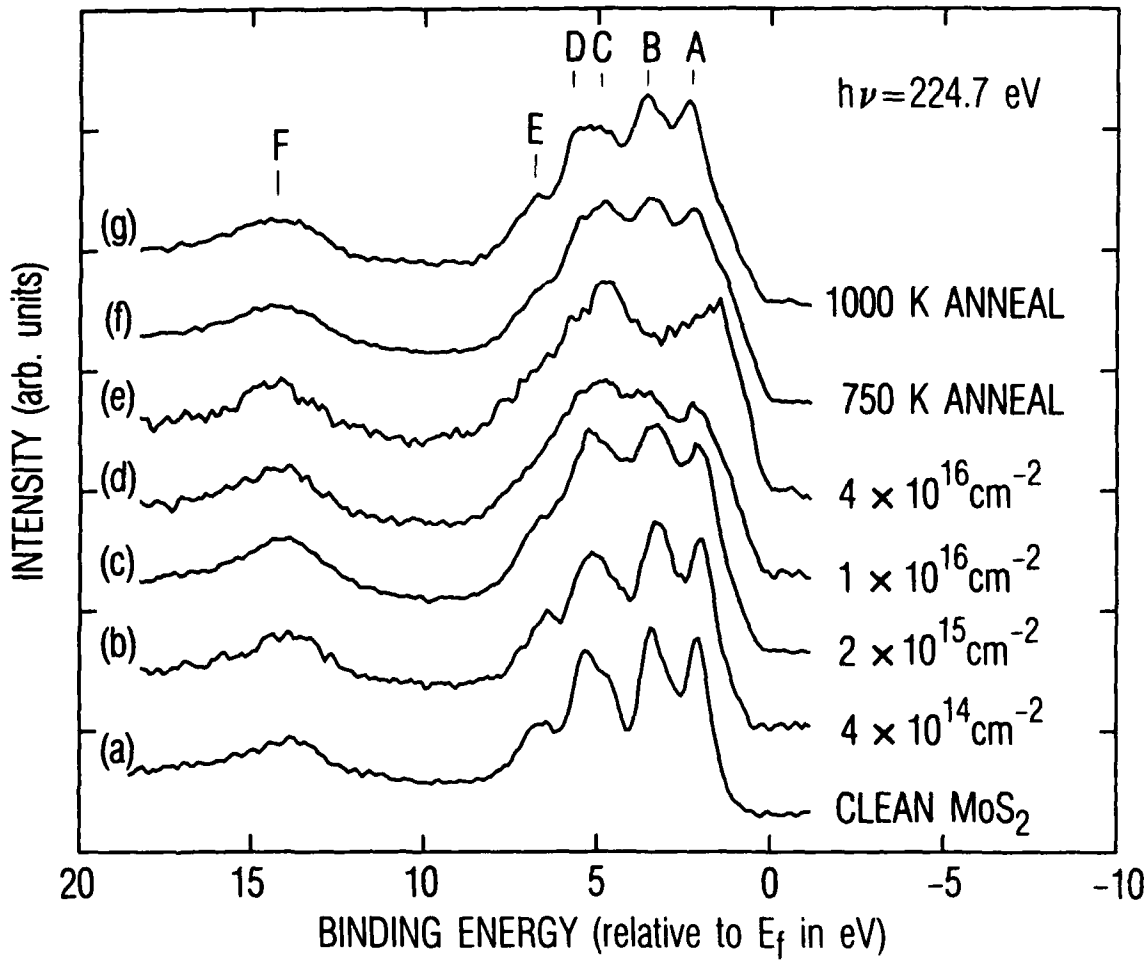

Fig. 3. Valence Band Spectra Produced Using a Photon Energy of 224.7 eV for the Same Conditions as in Fig. 1. The 224.7-eV photon energy represents the position of the Mo-3d x-ray absorption edge, resulting in a resonant enhancement of peak A and, to a lesser extent, peaks C and D. Hence, these spectra are more sensitive to chemical changes in the surface region than those for 152 eV (see Fig. 2).

the resonance spectrum, Fig. 3a), which shows that the electronic states involved in bonding in the surface region have increased Mo character. These changes are only partly due to the existence of the dispersed Mo(0), since the Mo(0) comprises only ~8% of the total Mo (see the core level spectra in Fig. 1) in the surface region for this Ne^+ fluence. The changes in the molecular orbital structure of MoS_2 during ion bombardment have been discussed in Ref. 20.

The lack of shifting of peaks A-E after bombardment at these relatively low fluences confirms that no significant band-bending is occurring, in agreement with the lack of shifting of the MoS_2 peaks in the Mo-3d and S-2p spectra. If band-bending was going to occur, it would have been complete after even the lowest fluence, since a relatively low density of defects can pin the Fermi level.

The valence band spectrum for the 1×10^{16} Ne^+/cm^2 bombardment (Fig. 2c) shows further broadening due to the presence of amorphous material and increased relative intensity in the area between peaks B and C. The large intensity in this area is probably due to the existence of Mo(0), since it accounts for over 60% of the total Mo for this Ne^+ fluence (see section 3.1). The continued existence of MoS_2 is shown by the persistence of peaks A and B. The shape of this spectrum is not consistent with bulk Mo being formed. If it were, the spectrum would begin showing a maximum ~ 2 eV below the Fermi level [23], rather than at ~4.5 eV, as in the present case.

The changes in the valence band spectra for the 224.7-eV photon energy cannot be interpreted as simply as for the 152-eV photon energy, since during bombardment, changes in the chemical state and structure of the surface can change the resonance effects. Therefore, the valence band spectra at 224.7-eV photon energy are more sensitive to changes in chemical state than the 152-eV spectra, since their shape is dependent on changes in resonance conditions in addition to changes in the valence band density of states. As for the 152-eV spectra, initial bombardment causes no large change in the relative peak positions in the spectra (see Fig. 3b). The

spectrum for the 1 × 10^{16} Ne^+/cm^2 bombardment (Fig. 3d) shows the existence of increased intensity centered at ~ 4.5 eV, and coexistence of the MoS_2 peaks, similar to the 152-eV spectrum (Fig. 2c). However, in the spectrum for the 4 × 10^{16} Ne^+/cm^2 bombardment (see Fig. 3e; no corresponding spectrum for 152 eV), there is no prominent evidence corresponding to the existence of MoS_2 (peaks A and B are not visible). This observation agrees with the core level spectrum (Fig. 1e), which shows a highly broadened Mo(IV) peak corresponding to the amorphous MoS_{2-x} region, representing only ~20% of the total Mo. The spectrum shows two broad features, at ~1.5 eV and at ~4.5 eV. The peak at ~1 eV might be partially due to some of the Mo(0) that has grown into large enough clusters to represent "bulk" Mo.

In the valence band spectra for both the 152- and 224.7-eV photon energies, the valence band maximum moves from ~1.0 eV below E_f for the clean surface (Figs. 2a and 3a), to E_f for bombardment fluences greater than ~ 1 × 10^{16} Ne^+/cm^2 (Fig. 2c, and Figs. 3c, 3d and 3e). This indicates that a metallic surface has been created that is probably caused by Mo(0) and defects in the MoS_2.

To summarize this section, valence band spectra at- and off- resonance ($h\nu$ = 224.7 eV and 152 eV, respectively) are consistent with the core level results. Specifically, increased Mo character is seen in the valence spectra, due at low bombardment (~ 4 × 10^{14} and ~ 2 × 10^{15} Ne^+/cm^2) to sulfur vacancy defects in the MoS_2, and at higher levels (~ 1 × 10^{16} Ne^+/cm^2) also due to Mo(0) clusters. For heavy ion fluences (~ 4 × 10^{16} Ne^+/cm^2), the spectra suggest the existence of a metallic surface consisting of Mo(0) interdispersed with an amorphized Mo-S region.

C. EFFECT OF ANNEALING ON CORE LEVELS

A sample that had been bombarded with 4 × 10^{16} Ne^+/cm^2 was annealed to 750 K for 10 min. There was no evidence of a LEED pattern after cooling down. This result indicates that the size of any crystalline areas of MoS_2 present after annealing was considerably less than the coherence length of LEED (~ 100Å). The Mo-3d spectrum (see Fig. 4c) shows two doublets that

are ~ 1.1 eV apart, corresponding with the shift expected between MoS_2 and metallic Mo [17]. Therefore, the Mo(0) particles have grown large enough to have increased ability for final-state relaxation.

The S-2p spectrum for the 750-K anneal (see Fig. 4g) deconvolutes clearly into two doublets. The larger, high-BE species is shifted ~0.2 eV to higher BE as compared to S(2-) in MoS_2, while the smaller low-BE species indicates the presence of sulfur with an oxidation state even smaller (i.e., more negative) than S in MoS_2. This latter species will be shown below to represent adsorbed sulfur. With a 1000-K anneal for 10 min for the same sample, the Mo(IV) doublet increases in size relative to the Mo(metal) doublet (see Fig. 4d), while the MoS_2 S(2-) doublet increases relative to the low-BE S doublet (see Fig. 4h). Finally, as for the case of the 750-K anneal, there was no evidence of crystallinity observed by LEED.

Comparison of the data for the annealed samples to those for the unannealed samples shows a decrease in the number of S species (i.e., less oxidation states), a large increase in the amount of reformed MoS_2, an increase in the separation between the Mo(IV) and Mo(0) species, and a drop in the Gaussian width of the Mo(IV) and S(2-) peaks (see Table I). These observations suggest that annealing caused movement of the system toward thermodynamic stability, promoted by high mobility of material on the surface. However, heating to these temperatures should be adequate to reproduce the original MoS_2(0001)-1 ×1 surface. For example, another semiconductor, GaAs, melts at 1511 K, which is higher than the melting point of MoS_2, 1458 K, but the crystallinity of its surface can be regenerated after low-energy ion bombardment for an anneal of only 800 K, which is 200 K below the highest heat treatment in the present study. In the present study, crystallinity is not completely restored because the anisotropic, layered crystal structure of MoS_2 results in its inability to promote mass diffusion perpendicular to the basal planes in the crystal. Small amounts of sulfur (in the form of polysulfide ion) can diffuse in this direction within the damaged layer due to high defect levels,

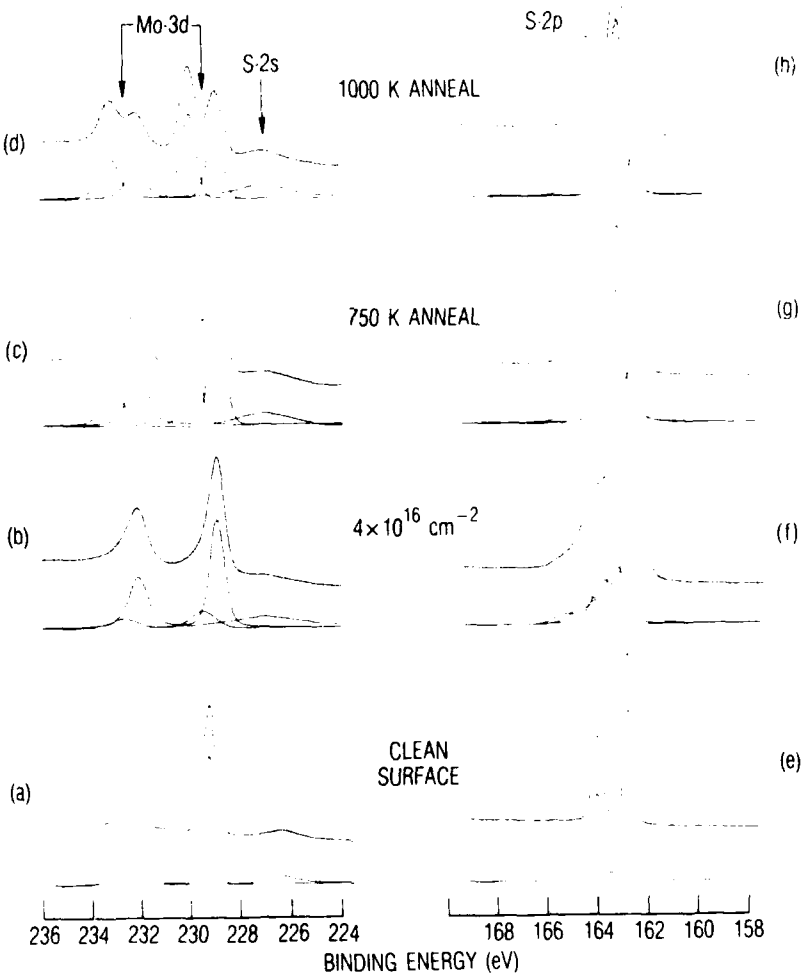

Fig. 4. Mo-3d and S-2p Core Level Spectra for the MoS_2(0001) Surface Representing the Effect of Annealing the Ne^+ Bombarded Surface. Spectra were taken with the same photon energies as for Fig. 1. Figs. (a) and (e) are for the clean MoS_2(0001) -1 × 1 surface (same as Figs. 1(a) and (f)), while (b) and (f) are for a Ne^+ fluence of 4×10^{16} Ne^+/cm^2 [same as Figs. 1(e) and (j)]. Figs. (c) and (g) represent a sample that had been annealed to ~ 750 K for 10 min after having been subjected to 4×10^{16} Ne^+/cm^2, while (d) and (h) are for the same sample annealed to ~ 1000 K for 10 min. Binding energies are relative to E_f.

resulting in the reformation of some of the MoS_2. However, most of the redistribution results from high mobility of species parallel to the surface. These observations suggest that producing well-ordered surfaces by ion bombardment and annealing cycles, a commonly used procedure with other materials, may not be possible for samples with highly two-dimensional crystal structures such as MoS_2.

The behavior of the valence band spectra upon annealing is consistent with the core level results. Upon annealing to 750 K (Fig. 3f), the MoS_2 peaks partially reappear. For the 1000-K anneal (Fig. 3g), they have approximately the same relative ratio as for the unbombarded samples. Also, their BEs are shifted ~ 0.2 eV higher as compared to those for the unbombarded surface, as are the corresponding peaks in the core level spectra (Figs. 4d and 4h). The sharp Fermi edge after the two anneals and the shoulder at ~ 1.5 eV are caused predominantly by the presence of metallic Mo.

To summarize this section, annealing a sample that had been bombarded with 4×10^{16} Ne^+/cm^2 to temperatures up to 1000 K resulted in flow of sulfur to the surface region in amounts that were inadequate to completely regenerate the $MoS_2(0001)$ ~1 × 1 surface. Core and valence spectra, along with LEED, indicate that, after annealing, the surface consists of MoS_2 and metallic Mo, with no long range order, i.e., a disordered surface.

D. VARIATION OF CHEMICAL STATE WITH DEPTH

As mentioned in section 2, the Mo-3d and S-2p core level spectra were also taken for electron kinetic energies of ~ 170 eV, as compared to ~ 70 eV for the spectra in Figs. 1 and 4. The resultant spectra were very similar to those in Figs. 1 and 4, except for differences in the relative heights of the various species in a spectrum (discussed below), and in Gaussian widths that were ~ 0.1 eV larger due to the change in the radiation line width from the monochromator, and, therefore, are not reproduced here.

Fig. 5 shows Mo(0):Mo(IV) peak area ratios for both the 70- and 170-eV electron kinetic energies. The Mo(0) species increases relative to the

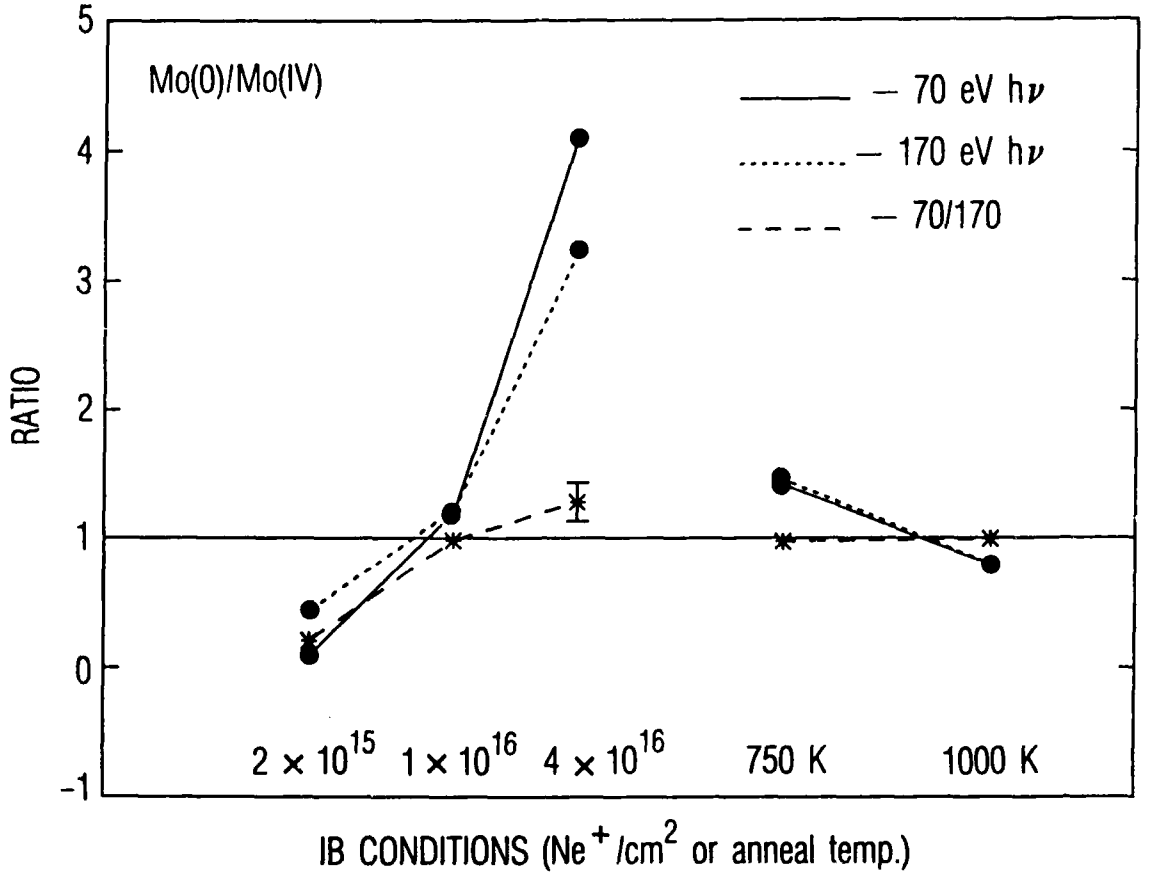

Fig. 5. Ratios of the Mo-3d Mo(0) Peak Area to the Mo(IV) Peak Area for Various Ion Fluences and Annealing Conditions. The ratios were determined for Mo-3d core levels taken at 300 and 400 eV, resulting in photoelectron kinetic energies of ~70 and ~170 eV, respectively. Also shown is the "70-eV/170 eV ratio", resulting in a qualitative depth profile of the variation of the relative ratio of these species in the surface region. Uncertainties in the 70-eV/170-eV ratio are smaller than the size of the symbols except where indicated by an error bar. Lines between points are drawn solely as an aid to the eye, and do not suggest linear variations of the ratios with ion fluence. (Data for the 4×10^{14} Ne^+/cm^2 fluence are not presented because of the inability to resolve the Mo(0) peak in the 170-eV spectrum.)

Mo(IV) species as fluence increases, as discussed in section 3.1. Fig. 5 also shows the ratio of these two ratios (i.e., the 70-eV Mo(0):Mo(IV) ratio divided by the 170-eV Mo(0):Mo(IV) ratio; denoted the "70-eV/170-eV ratio"). This quantity gives a qualitative measure of the depth distribution of the relative amounts of Mo species in the first ~10 Å of the surface. A ratio greater than 1 indicates enhancement of the Mo(0) species at the surface, while a ratio less than 1 indicates that Mo(0) is enhanced below the surface. Of course, the exact distribution as a function of depth cannot be mapped out and the distribution cannot be qualitatively determined for depths greater than ~ 10 Å for the electron kinetic energies in the present study. (The error bars for Figs. 5-7 are determined from the estimated uncertainty in the area of the peaks from the fitting procedure.)

Fig. 5 shows that with low bombardment levels ($\lesssim 2 \times 10^{15}$ Ne^+/cm^2), the Mo(0) is significantly enhanced below the surface. [This might explain the apparent drop in the Mo(0):Mo(IV) ratio between Figs. 1b and 1c. The reduced intensity might be due to the species being present below the detection depth of the technique rather than due to an actual decrease in the total Mo(0) present.] With 1×10^{16} Ne^+/cm^2, the Mo(0) is somewhat evenly distributed, while for 4×10^{16} Ne^+/cm^2, the Mo(0) is enhanced in the first few angstroms at the surface. The initial enhancement of the Mo(0) below the surface may be interpreted in terms of implantation of Mo atoms into the crystal during ion bombardment. This process can occur because the first-layer S atoms do not shadow the second-layer Mo atoms from the ions hitting the surface at the ion incidence angle of the present study.

The 70-eV/170-eV ratio for the annealed surface in Fig. 5 is 1.0 to a high precision for the anneals to both 750 K and 1000 K. This could either suggest the existence of unconnected Mo metal islands that were thicker than approximately twice the electron escape depth that formed on top of the disordered MoS_2 layer, or that MoS_2 and Mo metal coexist side-by-side on the surface. Of these two possibilities, the latter seems more probable,

since it is unlikely that there would be enough metallic Mo produced by ion bombardment and annealing that would form islands thicker than twice the escape depth and still cover enough of the surface to produce the large peaks in Figs. 4c and 4d.

Fig. 6 shows the polysulfide-S: MoS_2-S peak-area ratios for both the 70-and 170-eV electron kinetic energies. Similar to Fig. 5, the ratio becomes increasingly greater for fluences of 2×10^{15} to 4×10^{16} Ne^+/cm^2. The 70-eV/170-eV ratio suggests that for the 2×10^{15} and 1×10^{16} Ne^+/cm^2 bombardments, the polysulfide species is enhanced below the top few angstroms at the surface, while for the 4×10^{16} Ne^+/cm^2 bombardment, the polysulfide is spread fairly evenly through the top ~ 10 Å of the surface region.

The enhancement of polysulfide below the surface indicates that even though it may initially be distributed fairly evenly in the top 10 Å or so, the polysulfide on the surface was emitted/sputtered into the vacuum during the collision cascade. This observation may explain the preferential sputtering of sulfur over molybdenum during ion bombardment [1,2,4,5]. This supports a recent interpretation of preferential sputtering by Kelly [24], in which it was suggested that the species that are preferentially sputtered are the least chemically bound in the surface region. The polysulfide species are certainly bound less than metallic Mo or either the Mo or S in MoS_2 because less bonds to Mo are involved per S atom. This emission of sulfur could be driven by the high volatility of sulfur in the form of S_2, which could be formed easily from the $(S\text{-}S)^{2-}$.

Fig. 7 shows the ratio of the low-BE S peak to the S(2-) peak for the two anneals. The 70-eV/170-eV ratio shows that the low-BE S species is greatly enhanced at the top few angstroms at the surface. These species are probably adsorbed S species on the surface. Since MoS_2 does not adsorb species readily, especially at these annealing temperatures, this species is probably chemisorbed on the surface of the metallic Mo.

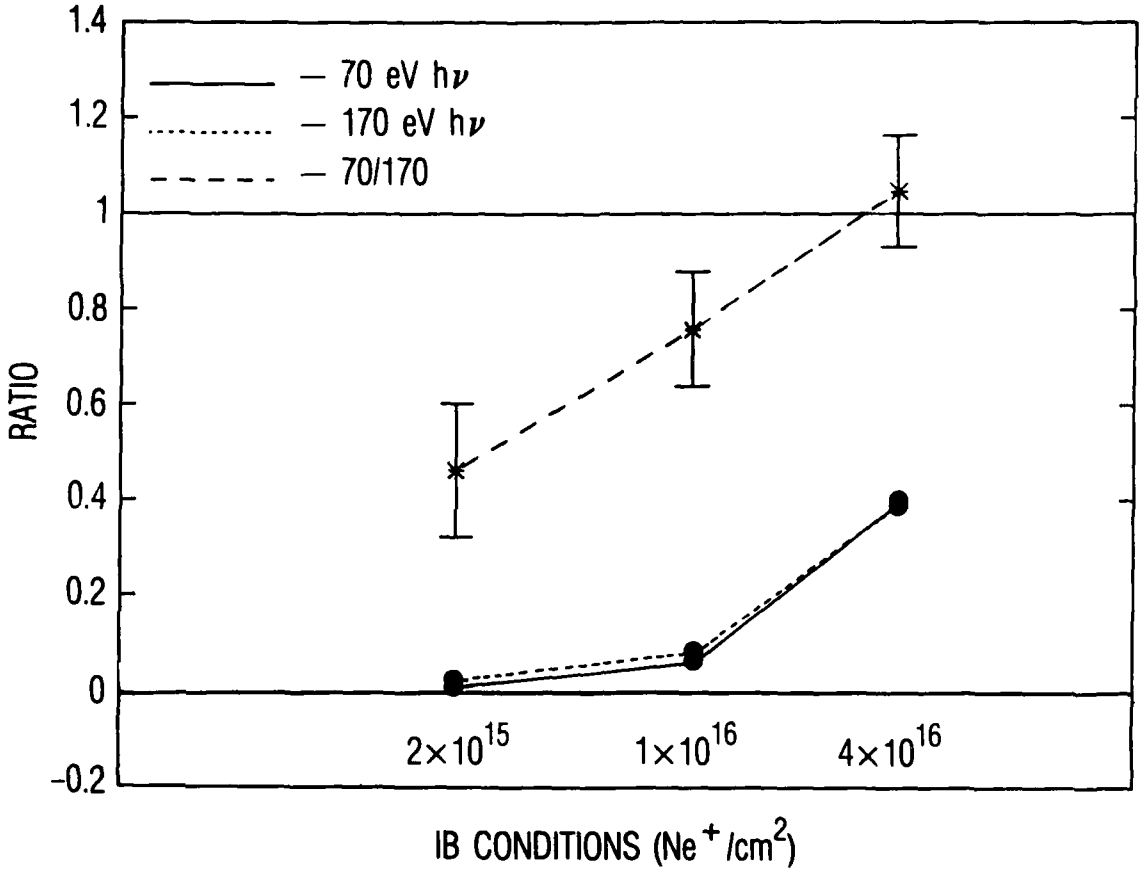

Fig. 6. Ratios of the "Polysulfide" Peak Area to the MoS_2 Sulfide Peak Area. The ratios were determined for S-2p core levels taken at 230 and 300 eV, resulting in photoelectron kinetic energies of ~70 and ~170 eV, respectively. Also shown is the ratio of the ~70-eV ratio to the ~170-eV ratio (see caption for Fig. 5).

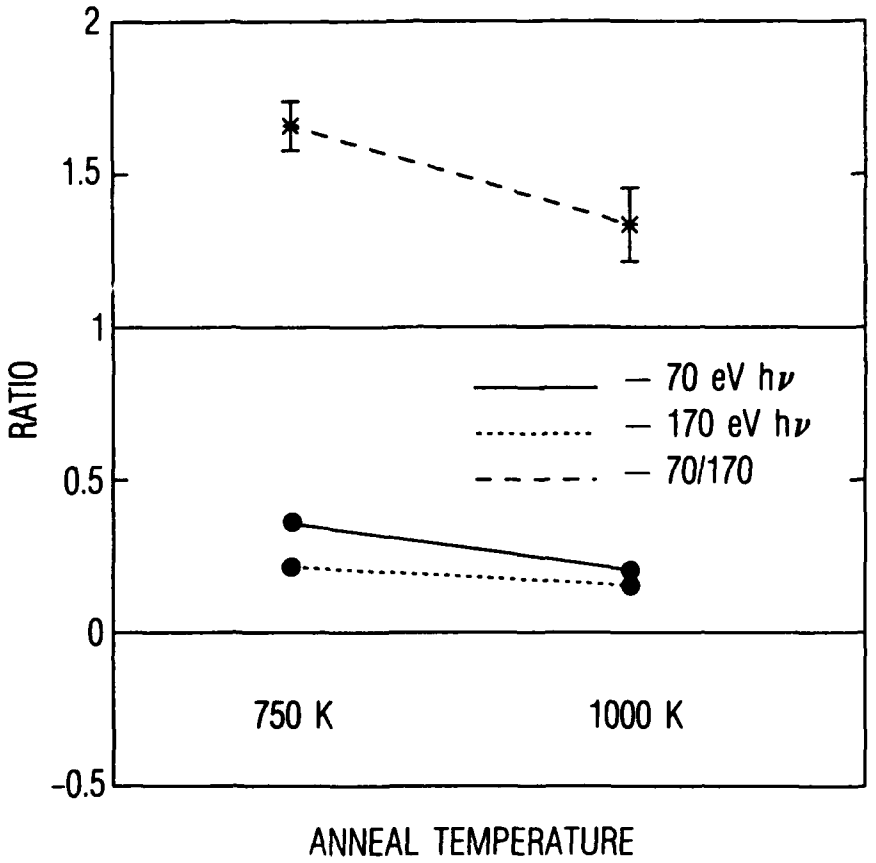

Fig. 7. Ratios of the Low-Binding-Energy S Peak Area to the MoS_2 Sulfide Peak Area for the Bombarded, Annealed Surface. Also shown is the ratio of the ~70-eV ratio to the ~170-eV ratio (see caption for Fig. 5).

In the work by Gellman, et al. [25], XPS was used to study the interaction of S adsorbed on a Mo(100) surface. They found an "S-2p" binding energy of 162.3 eV. Their study did not permit resolution of the 1/2 and 3/2 components, so their BE value corresponds to a weighted average of the positions of those two peaks. We computer-generated an S-2p spectrum with the approximate resolution of the study in Ref. 24. We calculated that the difference between the position of the peak maximum for the generated spectrum and the calculated value of the position of the 3/2 component was 0.4 eV. Therefore, the value for the S-$2p_{3/2}$ peak for adsorbed S on Mo(100) is probably ~161.9 eV. The expected binding energy for the S-$2p_{3/2}$ peak for MoS_2 is 162.3 eV [28], so that there is a shift to lower BE (~0.4 eV) for adsorbed S on Mo(100). This shift is approximately the same as for the low-BE S species in the present study (~0.5 eV), consistent with its assignment as adsorbed S.

To summarize this section, core level spectra of Mo and S taken for two electron kinetic energies, 70 and 170 eV, give qualitative depth distributions that can be used to suggest IB mechanisms. Initial bombardment (i.e., $<1 \times 10^{16}$ Ne^+/cm^2) causes enhancement of Mo(0) and $(S\text{-}S)^{2-}$ (polysulfide ion) below the surface. These effects are probably caused by implantation of Mo into the lattice producing the polysulfide, followed by emission of the polysulfide on the surface into the vacuum, and resulting in preferential sputtering of S over Mo at high fluences. Heavier bombardment (i.e., $>1 \times 10^{16}$ Ne^+/cm^2) results in these species being present in (relatively) greater amounts at the surface. Annealing a sample that had been bombarded with 4×10^{16} Ne^+/cm^2 showed that reformed MoS_2 clusters and metallic Mo clusters coexisted on the surface. A low-BE sulfur species is enhanced at the surface, indicating the presence of an adsorbed sulfur species on the surface of the metallic Mo.

IV. SUMMARY AND CONCLUSIONS

Exposure of the clean $MoS_2(0001)$-1 × 1 surface to 1-keV Ne^+ ions was studied with high-resolution photoelectron spectroscopy using synchrotron radiation. Analysis of Mo-3d and S-2p core levels showed that bombardment of the surface with $\lesssim 1 \times 10^{16}$ Ne^+/cm^2 resulted in production of Mo with a nominal oxidation state of zero that is dispersed in the MoS_2, and smaller amounts of a polysulfide species $[(S\text{-}S)^{2-}]$. For Ne^+ fluences of $\sim 4 \times 10^{16}$ Ne^+/cm^2, the surface region consisted mostly of the Mo(0) and small amounts of the $(S\text{-}S)^{2-}$ species, while the remaining Mo-S layer was highly amorphous and exhibited considerable S depletion as compared to MoS_2. Analysis of these core levels recorded with two different photoelectron kinetic energies showed that relative concentrations of the Mo(0) and polysulfide species were lower in the top few angstroms as compared to deeper layers for lower fluences, while, for the highest fluence, they were spread evenly throughout the top 10 Å in the surface region. The results suggest a chemical sputtering mechanism, supporting a recent theory on preferential sputtering by Kelly [24].

Valence band spectra taken for the same conditions agreed with the conclusions of the core level data. The movement of the valence band maximum toward the Fermi level suggests the production of a metal surface, even at lower ion fluences.

Annealing of the heavily bombarded (i.e., $\sim 4 \times 10^{16}$ Ne^+/cm^2) surface to 750 K followed by 1000 K did not result in the regeneration of an ordered $MoS_2(0001)$-1 × 1 surface as determined by LEED. Analysis of the core and valence spectra evinces the coexistence of MoS_2 and Mo metal in a disordered surface region, with S adsorbed on the surface of the Mo metal.

REFERENCES

[1] J. R. Lince, D. J. Carré, and P. D. Fleischauer, Langmuir 2 (1986) 805.

[2] J. R. Lince and P. D. Fleischauer, J. Vac. Sci. Technol. A5 (1987) 1312.

[3] J. R. Lince, et. al., Proc. Amer. Chem. Soc. Nat. Symp., Los Angeles, California, September, 1988.

[4] H. C. Feng and J. M. Chen, J. Phys. C7 (1974) 175.

[5] M. Kamaratos and C. A. Papageorgopoulos, Surf. Sci. 178 (1986) 865.

[6] S. M. Davis and J. C. Carver, Appl. Surf. Sci. 20 (1984) 193.

[7] M. Matsunaga, T. Homma, and A. Tanaka, ASLE Trans. 25 (1982) 323.

[8] S. M. Davis, private communication.

[9] J. C. McMenamin and W. E. Spicer , Phys. Rev. B16 (1977) 5474.

[10] J. Bandet, A. Malvand, and Y. Quemener, J. Phys. C13 (1980) 5657.

[11] L. A. Dietz and J. C. Sheffield, J. Appl. Phys. 46 (1975) 4361.

[12] F. J. Himpsel, Y. Jugnet, D. E. Eastman, J. J. Donelon, D. Grimm, G. Landgren, A. Marx, J. F. Morar, C. Oden, and R. A. Pollak, Nucl. Inst. Meth. 222 (1984) 107.

[13] D. E. Eastman, J. J. Donelon, N. C. Hien, and F. J. Himpsel, Nucl. Inst. Meth. 172 (1980) 327.

[14] Calculated from formula in S. Tanuma, C. J. Powell, and D. R. Penn, Surf. Sci. 192 (1987) L849, which was optimized for electron kinetic energies of about 200 eV and higher.

[15] P. R. Bevington, Data Reduction and Error Analysis for the Physical Sciences (McGraw-Hill, New York, 1969) p. 237.

[16] D. A. Shirley, Phys. Rev. B5 (1972) 4709.

[17] C. D. Wagner, W. M. Riggs, and L. E. Davis, Eds. J. F. Moulder and G. E. Mullenberg, X-ray Photoelectron Spectroscopy (Perkin-Elmer, Eden Prairie, MN, 1979).

[18] G. K. Wertheim, S. B. DiCenzo, and S. E. Youngquist, Phys. Rev. Lett. 51 (1983) 2310.

[19] K. S. Liang, S. P. Cramer, D. C. Johnston, C. H. Chang, A. J. Jacobson, J. P. deNeufville, and R. R. Chianelli, J. Non-Cryst. Solids 42 (1980) 345.

[20] I. Abbati, L. Braicovich, C. Carbone, J. Nogami, I. Lindau, and U. del Pennino, J. Electron Spectrosc. Related Phenomena 40 (1986) 353.

[21] P. D. Fleischauer, J. R. Lince, R. Bauer, and P. A. Bertrand, submitted to Langmuir.

[22] See, for example, L. C. Davis, J. Appl. Phys. 59 (1986) R25.

[23] S. J. Atkinson, C. R. Brundle, and M. W. Roberts, Chem. Phys. Lett. 24 (1974) 175.

[24] R. Kelly, Nucl. Instrum. Methods B18 (1987) 388.

[25] A. Gellman, W. T. Tysoe, F. Zaera, and G. A. Somorjai, Surf. Sci. 191 (1987) 271.

[26] G. C. Stevens and T. Edmonds, J. Catalysis 37 (1975) 544.

LABORATORY OPERATIONS

The Aerospace Corporation functions as an "architect-engineer" for national security projects, specializing in advanced military space systems. Providing research support, the corporation's Laboratory Operations conducts experimental and theoretical investigations that focus on the application of scientific and technical advances to such systems. Vital to the success of these investigations is the technical staff's wide-ranging expertise and its ability to stay current with new developments. This expertise is enhanced by a research program aimed at dealing with the many problems associated with rapidly evolving space systems. Contributing their capabilities to the research effort are these individual laboratories:

Aerophysics Laboratory: Launch vehicle and reentry fluid mechanics, heat transfer and flight dynamics; chemical and electric propulsion, propellant chemistry, chemical dynamics, environmental chemistry, trace detection; spacecraft structural mechanics, contamination, thermal and structural control; high temperature thermomechanics, gas kinetics and radiation; cw and pulsed chemical and excimer laser development including chemical kinetics, spectroscopy, optical resonators, beam control, atmospheric propagation, laser effects and countermeasures.

Chemistry and Physics Laboratory: Atmospheric chemical reactions, atmospheric optics, light scattering, state-specific chemical reactions and radiative signatures of missile plumes, sensor out-of-field-of-view rejection, applied laser spectroscopy, laser chemistry, laser optoelectronics, solar cell physics, battery electrochemistry, space vacuum and radiation effects on materials, lubrication and surface phenomena, thermionic emission, photosensitive materials and detectors, atomic frequency standards, and environmental chemistry.

Computer Science Laboratory: Program verification, program translation, performance-sensitive system design, distributed architectures for spaceborne computers, fault-tolerant computer systems, artificial intelligence, microelectronics applications, communication protocols, and computer security.

Electronics Research Laboratory: Microelectronics, solid-state device physics, compound semiconductors, radiation hardening; electro-optics, quantum electronics, solid-state lasers, optical propagation and communications; microwave semiconductor devices, microwave/millimeter wave measurements, diagnostics and radiometry, microwave/millimeter wave thermionic devices; atomic time and frequency standards; antennas, rf systems, electromagnetic propagation phenomena, space communication systems.

Materials Sciences Laboratory: Development of new materials: metals, alloys, ceramics, polymers and their composites, and new forms of carbon; nondestructive evaluation, component failure analysis and reliability; fracture mechanics and stress corrosion; analysis and evaluation of materials at cryogenic and elevated temperatures as well as in space and enemy-induced environments.

Space Sciences Laboratory: Magnetospheric, auroral and cosmic ray physics, wave-particle interactions, magnetospheric plasma waves; atmospheric and ionospheric physics, density and composition of the upper atmosphere, remote sensing using atmospheric radiation; solar physics, infrared astronomy, infrared signature analysis; effects of solar activity, magnetic storms and nuclear explosions on the earth's atmosphere, ionosphere and magnetosphere; effects of electromagnetic and particulate radiations on space systems; space instrumentation.